

Research Article

Acoustooptic Diffraction of Three-Color Radiation on a Single Acoustic Wave

V. M. Kotov  and S. V. Averin 

Kotel'nikov Institute of Radio Engineering and Electronics (Fryazino Branch), Russian Academy of Sciences, Fryazino, Moscow reg., 141190, Russia

Correspondence should be addressed to V. M. Kotov; vmk6054@mail.ru

Received 27 November 2018; Accepted 27 January 2019; Published 24 February 2019

Academic Editor: Sulaiman W. Harun

Copyright © 2019 V. M. Kotov and S. V. Averin. This is an open access article distributed under the Creative Commons Attribution License, which permits unrestricted use, distribution, and reproduction in any medium, provided the original work is properly cited.

Bragg diffraction which provides effective acoustooptic interaction of three-color radiation with a single acoustic wave at a high frequency of sound is proposed and tested in a single crystal of paratellurite at the wavelengths of $\lambda = 0.488, 0.514, \text{ and } 0.633 \mu\text{m}$. Maximal diffraction efficiency of radiation with $\lambda = 0.633 \mu\text{m}$ at acoustic frequency of 150 MHz is 88% and that with $\lambda = 0.488 \mu\text{m}$ and $\lambda = 0.514 \mu\text{m}$ is 60%. In diffraction efficiency range from 0 to 40% the dependence of all beams on acoustic power is the same.

1. Introduction

Acoustooptic (AO) diffraction is widely used to control the parameters of optical radiation. Bragg diffraction modes regimes, which allow deflecting radiation with efficiency close to 100%, turned out to be the most popular in practice [1, 2]. However, high selectivity of Bragg regime to the wavelength of light makes it difficult to use it to deflect multicolor optical radiation. It was shown that, in anisotropic materials, it is possible to deflect up to six beams with different wavelengths [3, 4]. However, sampling of the wavelengths is not random and optional sampling can be made only for two-color radiation [4]. This approach did find an application, in particular, in 2-dimensional laser anemometry [5, 6]. The task of controlling three-color optical radiation becomes acute in many areas of science and technology (see, e.g., [7–9]). As a rule, this problem is solved by using several AO-cells or by a single cell which is controlled by several acoustic frequencies [10]. Using only one AO-cell with a single acoustic frequency has several advantages: it eliminates the effects of intermodulation and reduces energy consumption, device size, and its cost, and so on.

For three-color radiation with an arbitrary set of wavelengths it is impossible to find the condition of strict Bragg synchronism with a single acoustic wave, but it is possible

to define the conditions when the Bragg mismatch would be minimal. A similar problem was previously tried to be solved in [11, 12] and practical realizations were found at ~ 84 and 87 MHz sound frequency. However, it is well known that the frequency of sound limits the range of measured speed in laser Doppler anemometry [13]. The operation principle of Doppler anemometry is based on the change of the light frequency after reflection from the moving object. Deviation of light frequency $\Delta\nu$ is defined from the relation $\Delta\nu/\nu = V/C$ where ν and C are frequency and speed of the light and V is speed of the moving object [14–16]. For example, change of $\Delta\nu = 100$ MHz corresponds to $V = 630$ m/s for the reflected light at the wavelength of $0.63 \mu\text{m}$. Laser Doppler anemometry based on the differential scheme allows measuring the value $\Delta\nu$ with respect to the frequency f of the acoustic wave which propagates through the AO crystal; in this case the relation $f > \Delta\nu$ has to be fulfilled. In other words, the higher the frequency of sound controlling the optical rays, the wider the measured velocity range. For 3-dimensional velocity measurements three beams with different wavelengths can be used, and then each velocity component is measured by one of the beams.

In this paper, we found the AO conditions for three-beam diffraction at the wavelength of $0.633 \mu\text{m}$ (He-Ne laser radiation), 0.488 , and $0.514 \mu\text{m}$ (Ar laser radiation) interacting with a “slow” acoustic wave propagating in a TeO_2

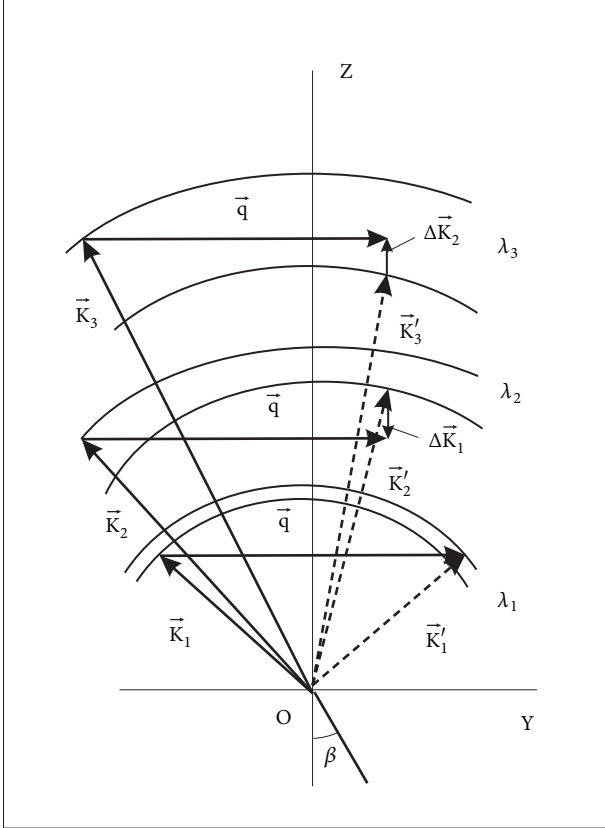


FIGURE 1: Vector diagram of the AO diffraction of three-color radiation.

crystal at the maximum possible frequency. The obtained acoustic frequency is ~ 150 MHz, which is almost twice the frequency of sound used previously.

2. Theory

Figure 1 shows a vector diagram of the proposed AO diffraction of three-color optical radiation on a single acoustic wave occurring in uniaxial positive gyrotropic crystal. It should be noted that the proposed regime can be realized in uniaxial crystals both with gyrotropy and without gyrotropy but we consider the gyrotropic crystal because we have in mind the gyrotropic paratellurite crystal. The optical light falls at an angle β on the input crystal face OY, oriented orthogonal to the optical axis OZ. The light splits inside the crystal onto the monochromatic components; each component in common case is represented by two beams with different polarizations. To avoid the picture overloading only one beam for each component which takes part in diffraction process is shown. The wave vectors of the incident optical radiation are \vec{K}_1, \vec{K}_2 , and \vec{K}_3 ; they represent the beams with wavelengths λ_1, λ_2 , and λ_3 , respectively ($\lambda_1 > \lambda_2 > \lambda_3$). All beams diffract on the single acoustic wave with the wave vector \vec{q} . The acoustic wave propagates orthogonal to the axis OZ. Only beam \vec{K}_1 is in strong Bragg synchronism with \vec{q} . Other beams \vec{K}_2 and

\vec{K}_3 diffract with small synchronism mismatch. The mismatch vectors are represented as $\Delta\vec{k}_1$ and $\Delta\vec{k}_2$; in a general case $\Delta\vec{k}_1 \neq \Delta\vec{k}_2$. All beams undergo anisotropic diffraction, that is, the diffraction with change of the wave vector surfaces. The diffracted beams are \vec{K}'_1, \vec{K}'_2 , and \vec{K}'_3 , respectively. The “ordinary” beam \vec{K}_1 diffracts into “extraordinary” beam \vec{K}'_1 (diffraction “o-e”). Other beams \vec{K}_2 and \vec{K}_3 diffract into \vec{K}'_2 and \vec{K}'_3 as “e-o” diffractions. In Figure 2 the mismatch Δk on the light wavelength λ is shown. It was assumed that the diffraction occurs in paratellurite on the shear and “slow” acoustic wave propagating orthogonal to the optical axis OZ with the velocity of 617 m/s. The calculations were made for the acoustic frequency 148 MHz and angle of incidence $\beta = 4.02^\circ$. By taking into account the crystal gyrotropy the refractive indices of the crystal are described by [17]:

$$\begin{aligned} & n_y^4 \left(\frac{1}{n_0^2 n_e^2} - G_{11}^2 \right) + n_z^4 \left(\frac{1}{n_0^4} - G_{33}^2 \right) \\ & + \frac{n_y^2 n_z^2}{n_0^2} \left[\left(\frac{1}{n_0^2} + \frac{1}{n_e^2} \right) - 2G_{11}G_{33}n_0^2 \right] - 2\frac{n_z^2}{n_0^2} \\ & - n_y^2 \left(\frac{1}{n_0^2} + \frac{1}{n_e^2} \right) + 1 = 0, \end{aligned} \quad (1)$$

where n_y and n_z are the projections of the refraction vector \vec{n} on the OY and OZ directions, respectively (the direction of the refraction vector \vec{n} coincides with the light wave vector \vec{K} , and its value is equal to the refractive index of the crystal [18]), n_0 and n_e are the principal refractive indices of the crystal, and G_{11} and G_{33} are the components of the pseudogyration tensor. In our calculations the influence of G_{11} was neglected, it was assumed that $G_{11} = 0$. The refractive indices and the component G_{33} for the TeO₂ as the functions of wavelength λ are derived from [19–21] and can be written as

$$\begin{aligned} n_0 &= \frac{7.76658 \cdot 10^{-10}}{\lambda^2} - \frac{11.9507 \cdot 10^{-6}}{\lambda} + 2.253, \\ n_e &= \frac{9.337 \cdot 10^{-10}}{\lambda^2} - \frac{14.7035 \cdot 10^{-6}}{\lambda} + 2.409, \\ G_{33} &= \frac{3.9442 \cdot 10^{-22}}{\lambda^4} - \frac{1.7037 \cdot 10^{-17}}{\lambda^3} + \frac{2.7725 \cdot 10^{-13}}{\lambda^2}. \end{aligned} \quad (2)$$

The projections of the wave vector \vec{K} on the directions OY and OZ are equal accordingly to $K_y = (2\pi/\lambda)n_y$ and $K_z = (2\pi/\lambda)n_z$. In Figure 2 two branches which correspond to diffractions “o-e” and “e-o” are shown. It can be seen that, with the parameters mentioned above, the beam with a wavelength $\lambda_1 = 0.633 \mu\text{m}$ is in strong Bragg synchronism, $\Delta k = 0$, but for other beams with $\lambda_2 = 0.514 \mu\text{m}$ and $\lambda_3 = 0.488 \mu\text{m}$ $\Delta k \sim 5 \text{ cm}^{-1}$. Figure 3 shows a dependency of Δk from angle β for the before-mentioned wavelengths at acoustic frequency of 148 MHz. As evident $\Delta k = 0$ for the light

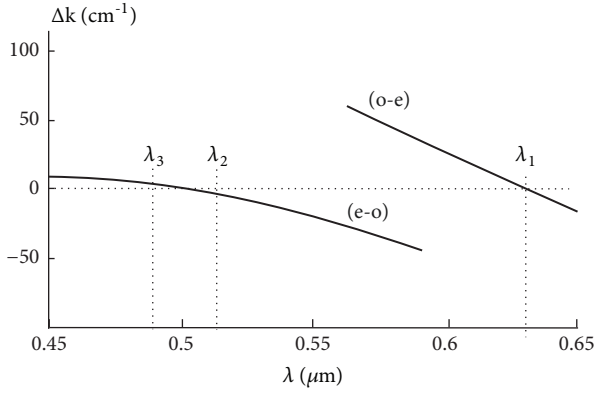


FIGURE 2: Mismatch $\Delta \vec{k}$ as a function of the light wavelength λ .

with λ_1 at $\beta = 4.02^\circ$; for other beams Δk does not exceed 5 cm^{-1} . This Δk value gives rise to the theoretical maximal diffraction efficiency not less than 65% at AO-interaction length equal to 0.4 cm (experimental conditions, see below). Figure 4 represents the theoretical dependencies of the 1st order diffraction efficiency η on the electrical power which is applied to the piezo transducer as well as the experimental results. The theoretical curves are calculated according to (3) [1, 2]:

$$\eta = \frac{I_1}{I_{\text{inc}}} = \frac{v^2}{(\Delta k L)^2 + v^2} \sin^2 \left[0.5 \sqrt{(\Delta k L)^2 + v^2} \right], \quad (3)$$

where I_1 is intensity of the beam diffracted into the 1st order, I_{inc} is intensity of the incident beam, v is Raman-Nath parameter, $v \approx (2\pi/\lambda) \sqrt{(M_2 L/2H) P_{\text{ac}}}$ where λ is wavelength of the light, M_2 is AO figure of merit, L and H are length of AO-interaction and the height of the acoustic column, and P_{ac} is the acoustic power. In our calculations $L = H = 0.4$ cm (experimental conditions) and M_2 was taken equal to $1200 \times 10^{-18} \text{ s}^3/\text{g}$. According to our measurements $P_{\text{ac}} = 0.64 P$, where P is electrical power applied to the piezo transducer. It is clearly seen that at initial stage ($P < 50$ mW) the curves for different wavelengths are located quite near to each other. At $P > 100$ mW these dependences start to diverge significantly. In our experiments (see below) the conditions of linear dependence of all beams in wide range of the variation of applied electrical power were achieved at acoustic frequency ~ 150 MHz.

2.1. Experiment. For testing of our approach the experiment has been performed. The experimental setup is presented in Figure 5. Ar laser 1 generates two bright beams at $\lambda_2 = 0.514 \text{ } \mu\text{m}$ and $\lambda_3 = 0.488 \text{ } \mu\text{m}$. These beams propagate through attenuator 2, quarter-wave plate 3, and then pass through a splitter 4. At the same time beam with wavelength $\lambda_1 = 0.633 \text{ } \mu\text{m}$ generated by laser 5 goes through quarter-wave plate 6 and then is reflected from plate 4. After plate 4 all beams propagate collinearly with respect to each other. The surfaces of plate 4 have special coating; therefore beams λ_2 and λ_3 pass through this plate but beam λ_1 is reflected from it. The total radiation modulates by mechanical chopper 7 and focuses on

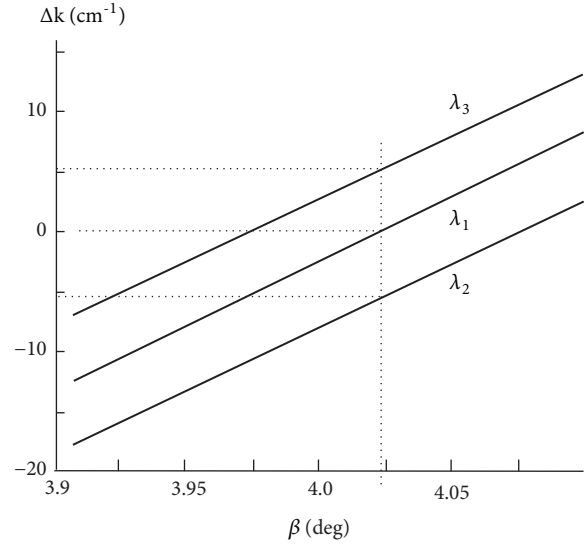


FIGURE 3: The dependence of mismatch $\Delta \vec{k}$ from the incident angle β at the acoustic frequency $f = 148$ MHz.

the AO-cell 8 which is made of TeO_2 crystal. The dimensions of the cell are $10 \times 10 \times 8 \text{ mm}^3$ along the directions $[110]$, $[1\bar{1}0]$, and $[001]$, respectively. The input and output optical faces of the AO-cell have the antireflection coatings and the reflection losses of all beams were less than 0.5%. The direction OY in Figure 1 corresponds to the $[110]$ direction and optical axis OZ corresponds to $[001]$ direction. The piezo transducer from LiNbO_3 is bonded to the face $\{110\}$ and generates the shear acoustic wave in the frequency range of 140...155 MHz. The sound velocity in TeO_2 crystal is 617 m/s.

The intensities of the initial laser beams propagating in I_0 direction without acoustic wave were measured by means of photodetector. During the measurement the beams were separated from each other with the interference filters. Intensities of the beams at the wavelengths of λ_1 , λ_2 , and λ_3 were 15, 25, and 15 mW, correspondently. Diffracted beams were measured when the acoustic wave was propagated through the crystal. Diffraction efficiency was defined as the ratio of the intensities of the diffracted and incident beams. A set of the calibrated optical attenuators was used to increase the measurement accuracy. All diffracted beams propagate on one side with respect to the incident beam. Since the beams λ_2 and λ_3 propagate fairly close to each other, the interference filters 10 were used to separate them. No filter was required for extracting the beam λ_1 .

Figure 4 demonstrates the experimental results for the wavelengths of $0.633 \text{ } \mu\text{m}$, 0.514 , and $0.488 \text{ } \mu\text{m}$. Maximum diffraction efficiency of radiation with $\lambda = 0.633 \text{ } \mu\text{m}$ at acoustic frequency of 150 MHz is 88% and that with $\lambda = 0.488 \text{ } \mu\text{m}$ and $\lambda = 0.514 \text{ } \mu\text{m}$ is 60%. The most interesting from a practical point of view is the existence of a range in the initial section of Figure 4 when the intensities of all beams change linearly and the slope of all curves is the same. Here beams intensities vary up to 40% of the incident radiation.

It should be noted that if all the incident beams were in strict Bragg synchronism with the acoustic wave, that is, condition $\Delta k = 0$ is fulfilled, then, as follows from (3), the

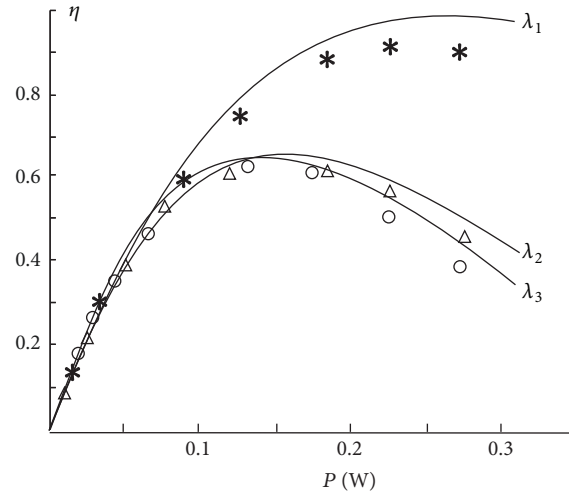


FIGURE 4: Diffraction efficiency η as a function of the electrical power P . Experimental results for the wavelengths of $0.633 \mu\text{m}$, 0.514 , and $0.488 \mu\text{m}$ are indicated as (*), (Δ), and (o), respectively.

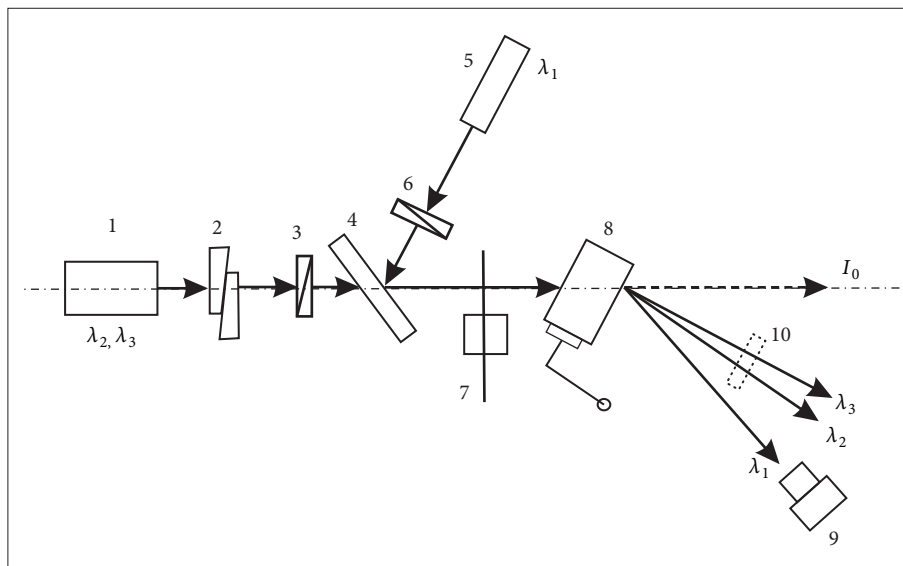


FIGURE 5: Optical scheme of the experimental setup.

slopes of all the curves in the initial section of Figure 4 would be different. All our experiments confirmed the theoretical conclusions; good agreement was obtained between the experimental and the theoretical results. The optimal experimental frequency of 150 MHz practically coincides with the theoretical one of 148 MHz.

2.2. Conclusion. In this paper we have proposed and examined a variant of AO diffraction of three-color optical radiation on a single acoustic wave at the maximum possible frequency of transverse sound propagating orthogonally to the optical axis of the TeO_2 crystal. To obtain effective diffraction of optical beams on given wavelengths it was proposed to use diffraction regimes with mismatched Bragg synchronism. According to the developed method the diffraction conditions were chosen so that the radiation beam with the maximum wavelength was in strict Bragg synchronism with the acoustic wave, whereas the dissynchronism of the

other beams with the same acoustic wave was minimal. The presence of equal dependence of diffraction efficiency of the beams at wavelengths of 0.633 , 0.514 , and $0.488 \mu\text{m}$ on the acoustic power has been revealed. Variation of beam intensities was linear, with equal slope, and may change from 0 to 40% of the incident radiation. The proposed technique has been demonstrated on the example of three-color radiation, two beams of which (0.488 and $0.514 \mu\text{m}$) are generated by an Ar laser and the third beam ($0.633 \mu\text{m}$) is generated by a He-Ne laser. The beams interact with a single acoustic wave propagating in a paratellurite crystal with the velocity of 617 m/s. It has shown that the optimal regime is realized when using a paratellurite crystal at the acoustic frequency of 150 MHz. In this case the maximum diffraction efficiency with a wavelength of $0.633 \mu\text{m}$ is 88%, and with wavelengths 0.488 and $0.514 \mu\text{m}$ it is 60%.

The results obtained can be used to elaborate new AO devices designed to control three-color laser radiation.

Data Availability

Data sharing is not applicable to this article as no datasets were generated or analyzed during this current study.

Conflicts of Interest

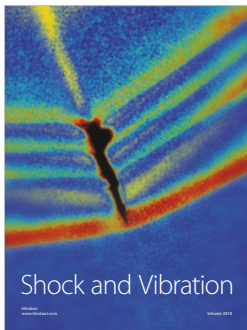
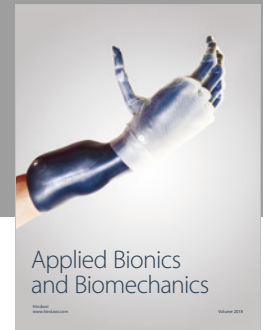
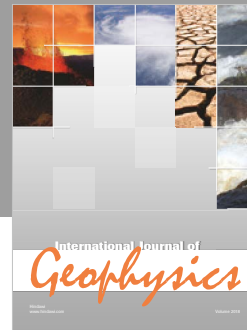
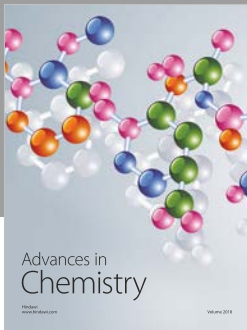
The authors declare that they have no conflicts of interest.

Acknowledgments

This work is partially supported by RFFI (Russian Fund of Fundamental Investigations), Grants no. 18-07-00259 and no. 19-07-00071.

References

- [1] V. I. Balakhshij, V. N. Parygin, and L. E. Chirkov, *Physical Principles of Acousto-Optics*, Radio & Svyaz, 1985.
- [2] J. Xu and R. Stroud, *Acousto-Optic Devices: Principles, Design and Applications*, John Wiley & Sons, Inc., New York, NY, USA, 1992.
- [3] V. M. Kotov and G. N. Shkerdin, "Acoustooptical diffraction of multicomponent optical radiation from a single acoustic wave in uniaxial crystals," *Optics and Spectroscopy*, vol. 85, no. 1, pp. 118–122, 1998.
- [4] V. M. Kotov, "Acousto-Optics," Bragg diffraction of the Multi-Color Radiation (Yanus-K, 2016).
- [5] S. N. Antonov, V. M. Kotov, and V. N. Sotnikov, "Bragg polarization splitters of the light on the basis of the crystal TeO₂," *Journal of Technical Physics*, vol. 61, no. 1, pp. 168–173, 1991.
- [6] V. M. Kotov and G. N. Shkerdin, "Acousto-optical splitters – frequency shifters for two-coordinate laser anemometers," *Acoustical Physics*, vol. 40, no. 2, pp. 309–310, 1994.
- [7] A. Henrie, B. Haymore, and D. E. Smalley, "Frequency division color characterization apparatus for anisotropic leaky mode light modulators," *Review of Scientific Instruments*, vol. 86, no. 023101, 2015.
- [8] J.-C. Kastelik, K. B. Yushkov, S. Dupont, and V. B. Voloshinov, "Cascaded acousto-optical system for the modulation of unpolarized light," *Optics Express*, vol. 17, no. 15, pp. 12767–12776, 2009.
- [9] J.-C. Kastelik, J. Champagne, S. Dupont, and K. B. Yushkov, "Wavelength characterization of an acousto-optic notch filter for unpolarized near-infrared light," *Applied Optics*, vol. 57, no. 10, pp. C36–C41, 2018.
- [10] M. G. Gazalet, G. Waxin, J. M. Rouvaen, R. Torguet, and E. Bridoux, "Independent acoustooptic modulation of the two wavelengths of a bichromatic light beam," *Applied Optics*, vol. 23, no. 5, pp. 674–681, 1984.
- [11] V. M. Kotov, "Bragg diffraction of three-color radiation in a paratellurite crystal," *Acoustical Physics*, vol. 61, no. 6, pp. 665–668, 2015.
- [12] V. M. Kotov, G. N. Shkerdin, A. N. Buliuk, A. I. Voronko, and S. A. Tichomirov, "Bragg diffraction of four-color optical radiation," *Radiotekhnika*, vol. 8, pp. 53–57, 2015.
- [13] F. Durst, A. Melling, and J. H. Whitelaw, *Principles and Practices of Laser-Doppler Anemometry*, Academic Press, 1981.
- [14] J. Zhou, W. Yang, and X. Long, "Research on multipoint layer-type laser Doppler self-velocimeter," *Optical Engineering*, vol. 49, no. 4, p. 044301, 2010.
- [15] K. Maru and T. Hata, "Nonmechanical scanning laser Doppler velocimeter for cross-sectional two-dimensional velocity measurement," *Applied Optics*, vol. 51, no. 34, pp. 8177–8183, 2012.
- [16] X. Zhang, W. Gu, C. Jiang, B. Gao, and P. Chen, "Velocity measurement based on multiple self-mixing interference," *Applied Optics*, vol. 56, no. 23, pp. 6709–6713, 2017.
- [17] V. M. Kotov, S. V. Averin, E. V. Kotov, and G. N. Shkerdin, "Acousto-optic filters based on the superposition of diffraction fields [Invited]," *Applied Optics*, vol. 57, no. 10, pp. C83–C92, 2018.
- [18] F. I. Fyodorov, *Optics of Anisotropy Media*, URSS, Moscow, Russia, 2004.
- [19] M. P. Shaskol'skaya, Ed., *Acoustical Crystals*, Nauka, Moscow, Russia, 1982.
- [20] V. A. Kizel and V. I. Burkov, *Gyrotropy of Crystals*, Nauka, Moscow, Russia, 1980.
- [21] V. Y. Molchanov, Y. I. Kitaev, A. I. Kolesnikov et al., *Theory and Practice of the Modern Acoustooptics*, MISiS, 2015.



Hindawi

Submit your manuscripts at
www.hindawi.com

